

Article

Microstructural regulation of seasonal organic nitrate accumulation on pine needle surfaces

Xinze Yan^{*}, Jinyan Cai, Mengmeng Chen, Jianjiang Lu^{*}

School of Chemistry and Chemical Engineering, Shihezi University, Shihezi 832003, China

^{*} **Corresponding authors:** Xinze Yan, yanxinze2022@163.com; Jianjiang Lu, lujianjiang2021@163.com

CITATION

Yan X, Cai J, Chen M, Lu J.
Microstructural regulation of
seasonal organic nitrate accumulation
on pine needle surfaces. *Molecular &
Cellular Biomechanics*. 2025; 22(5):
1725.
<https://doi.org/10.62617/mcb1725>

ARTICLE INFO

Received: 28 February 2025

Accepted: 30 May 2025

Available online: 19 June 2025

COPYRIGHT



Copyright © 2025 by author(s).

Molecular & Cellular Biomechanics

is published by Sin-Chn Scientific

Press Pte. Ltd. This work is licensed

under the Creative Commons

Attribution (CC BY) license.

<https://creativecommons.org/licenses/by/4.0/>

Abstract: This study investigates the microregulatory mechanisms governing seasonal variations in particle-bound organic nitrates (PBONs) accumulation on pine needle surfaces. Using scanning electron microscopy, atomic force microscopy, and high-resolution mass spectrometry across five sites in the Changbai Mountain Nature Reserve, we revealed that seasonal transformations in epicuticular wax properties directly control PBON retention. Winter conditions produced maximum wax thickness ($5.82 \pm 0.47 \mu\text{m}$) and PBON concentrations ($142.6 \pm 18.3 \text{ ng/g}$), while summer showed minimums for both ($2.73 \pm 0.55 \mu\text{m}$; $56.4 \pm 9.7 \text{ ng/g}$). We identified temperature as the dominant environmental factor ($r = -0.81$) with a previously unreported threshold effect at $4.8 \text{ }^\circ\text{C}$, below which PBON accumulation rates accelerate significantly. Structural equation modeling revealed that seasonal conditions influence PBON accumulation through both direct atmospheric pathways and surface-mediated mechanisms. The findings demonstrate that microstructural changes in sampling surfaces are crucial for interpreting seasonal biomonitoring data and understanding pollutant dynamics in forest ecosystems.

Keywords: particle-bound organic nitrates (PBONs); pine needles; seasonal variation; epicuticular wax; microstructure; biomonitoring

1. Introduction

Particle-bound organic nitrates (PBONs), have attracted much interest because of their relevance in atmospheric chemistry as well as in terms of human health [1]. The semi-volatiles with $-\text{ONO}^2$ functional group are emitted both via direct emissions and gas-phase second-order chemistry. Therefore, PBONs plays a critical role in particulate pollution, nitrogen cycling, tropospheric ozone formation, and climate forcing.

Coniferous needles have served as effective bioindicators as well as passive collectors in monitoring aerial pollutants, such as PBONs, due to surface properties as well as extensive distribution [2]. The existence of a waxy cuticle forms a perfect substrate on which aerial particles tend to collect, whereas its extended residence time between 2 and 5 years makes it a suitable medium on which longitudinal pollution monitoring can be conducted, making it different from active collectors.

The efficacy of pine needles as PBON samplers shows significant temporal variability, attributed to seasonal environmental fluctuations. Changes in temperature, humidity, precipitation, and solar radiation can alter both pine needle surface properties and PBON atmospheric behavior [3]. These variations modify needle microstructural characteristics, including stomatal density, epicuticular wax composition, and cuticular permeability, influencing sorption kinetics and partition

equilibrium of organic pollutants. Despite recognizing these seasonal factors, the underlying molecular mechanisms governing seasonal PBON accumulation patterns on coniferous surfaces remain inadequately understood [4].

This study sheds light at a microscopic level on the pathways that determine the coverage of pine needles with PBONs. Using a novel combination of microscopic visualization methods with extensive chemical examination, we determine quantitative relationships between annually varying environmental variables, surface micromorphology, and distribution regimes of PBONs. Unveiling these pathways improves molecular understanding of surface-cosolvent interfaces, allows more insightful interpretation of bioassessments, and helps in the development of advanced models with reference to environmental pollutants.

2. Materials and methods

2.1. Study area and sample site design

This research focused on the Changbai Mountain National Nature Reserve located in the northeast of China ($41^{\circ}41'–42^{\circ}51' N$, $127^{\circ}42'–128^{\circ}16' E$) (**Figure 1**). It was selected due to its mountainous region of northeastern China containing rich coniferous forest ecosystems that have been less anthropogenically disturbed than other areas, making it appropriate for studying organic nitrate particles PBONs seasonal change dynamics [5]. The reserve contains varied vegetation zones, such as a belt of mixed broadleaf-conifer forests between 700 and 1100 m of altitude, where the dominant coniferous species is *Pinus koraiensis*, which extends from 740 m to 2691 m above sea level.

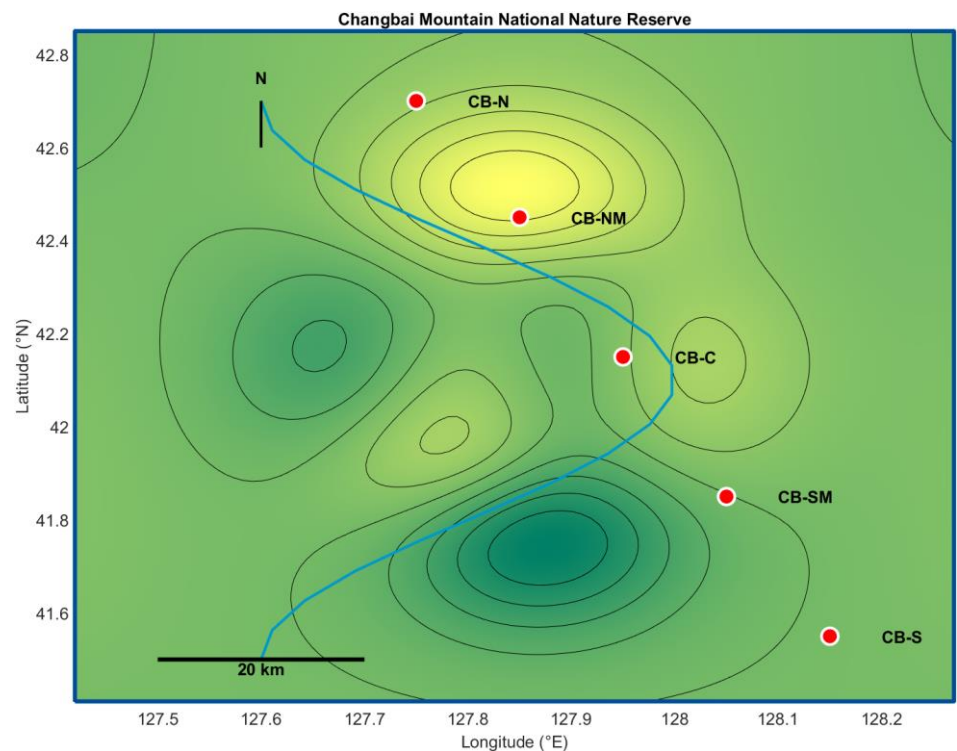


Figure 1. Geographic location of the changbai mountain national nature reserve.

Note: The map displays the distribution of five sampling sites (CB-N, CB-NM, CB-C, CB-SM, and CB-S) across the reserve. Base maps from the Natural Earth database, generated using MATLAB R2021b.

In order to evaluate possible differences in meteorological conditions and atmospheric deposition from north to south within the reserve, five sampling points were positioned within a north-south transect (**Figure 1**). These sites were identified as CB-N (northern boundary), CB-NM (northern middle), CB-C (center), CB-SM (southern middle), and CB-S (southern boundary), with the neighboring sites located laterally at a distance of 15–20 km from one another [6]. The selection of each sampling site was done using the following conditions: (1) a minimum of 2 km distance from roads or settlements to reduce anthropogenic direct impacts, (2) 25%–35% forest canopy cover that can reasonably represent atmospheric deposition, (3) approximately 80–100-year-old *Pinus koraiensis* stands of specified age and density, and (4) accessible for fieldwork throughout all seasons for sampling campaign needs [7].

In each site, a rectangular plot of 50 × 50 m was established within which five mature needles of *Pinus koraiensis* were collected at random. The estimated age of these trees is 85–95 years, as per increment core analysis. Their height (23–28 m) and crown development were also approximately uniform. Marking and georeferencing were carried out for each tree with a high-precision GPS (Trimble GeoXT 6000, accuracy ±0.5 m) to ensure that the samples across the study were longitudinally consistent over time [8].

In order to encompass the entire complexity of seasonal environmental changes, seasonal sampling campaigns were conducted within the middle month of each meteorological season, specifically October (autumn), January (winter), April (spring), and July (summer) within the range of 2022 to 2023. Full meteorological data were collected for each event using portable weather stations (Davis Vantage Pro2, Davis Instruments, USA) installed at each site, which recorded temperature, relative humidity, precipitation, wind speed, wind direction, and solar radiation every 30 min during the sampling periods.

2.2. Pine needle sampling protocol

Pine needles were harvested according to a defined protocol that aimed to maintain sampling uniformity across all events and locations [9]. At each location, current-year (C) and one-year-old (C + 1) needles were taken from five predetermined *Pinus koraiensis* trees. To reduce possible within-canopy heterogeneity variation, samples were taken mid-crown from a height of 15–18 m on a south-facing side using telescopic pruners [10]. With respect to each tree, needle clusters were collected from different branches, while avoiding those exhibiting signs of herbivory, disease, or physical damage.

Approximately 50 g of needles were collected from each tree per age class, totaling 10 samples per site per sampling period. Sampling was done on non-rainy days and at least 48 h after the last precipitation event to minimize the effect of washout and wet deposition on PBONs [11]. All samples were collected between 09:00 and 15:00 local time to eliminate the possibility of diurnal variation in stomatal behavior and surface wax features.

During transfer to the laboratory, the samples were stored in portable refrigerators at 4 degrees Celsius while being labeled with unique identifiers consisting of a site

code, tree number, needle age class, and collection date. All sampling equipment was cleaned with methanol between trees in order to prevent cross-contamination. Within 24 h of collection, the samples were transferred into the laboratory, where they underwent a gentle rinsing procedure to remove loose particles using ultrapure water. After that, the samples were dried for 24 h at room temperature in a laminar flow hood to prevent contamination, and then stored at -20 degrees Celsius until further analysis was to be carried out. The field blanks were made by opening the pre-cleaned plastic bags and letting them sit in the outside air for as long as the duration of the actual sampling process.

2.3. Laboratory analysis methods

2.3.1. Microscopic observation of pine needle surface structure

In this case, a pine's surface microstructure was analyzed by deep scanning electron microscopes and atomic force microscopes in order to monitor the different seasonal changes in its features [12]. For SEM analysis, the needle samples from four seasons were 5 mm segments cut from the middle portion of individual needles, which were prepared with a fixed procedure that included 24 h fixing in 2.5% glutaraldehyde, dehydrating by ethanol gradient, and then critical point drying. The gold sputter coating thickness prior to scanning electron microscope analysis was 10 nm, and the operational voltage was set to 5 kV, using Quorum K850 UK as the drying equipment instead.

3000X ten random stomatal areas were selected per sample, out of which unique particulate matter deposition patterns, stomata wax reticulated crystalloid formations, and glaucosphere wax were analyzed. Stomatal openness was assessed through ImageJ software, and it was calculated as a quantity for the area of one square millimeter. Epicuticular wax was documented with other covers following set rules and their area was analyzed quantitatively [13].

Additionally, the SEM observations were supplemented with an AFM (Atomic Force Microscope) analysis for further examination of the surface topography and nano-scale features. Fresh needle samples were sectioned into 1-centimeter pieces and quickly mounted onto magnetic discs with double-sided adhesive tapes. AFM imaging was performed with a Bruker Dimension Icon system in tapping mode using silicon probes with a nominal spring constant of 40 N/m and a resonance frequency of 300 KHz. The spring constant of each probe was calibrated before use using the thermal tune method following the manufacturer's protocol, with measured values typically within $\pm 5\%$ of the nominal value. Calibration was verified using a reference sample of known hardness (highly oriented pyrolytic graphite) to ensure measurement accuracy and data reliability. Surface scanning was accomplished with simultaneous acquisition of height, amplitude, and phase images as a sequence of $20 \times 20 \mu\text{m}$ and $5 \times 5 \mu\text{m}$. The surface roughness parameters like arithmetic average roughness, Ra, root mean square roughness, Rq, and maximum height, Rmax, were calculated with the manufacturer's software, NanoScope Analysis 1.9.

For each seasonal sampling period, all optical micrographs were made on needles of the current year (C) and one-year-old needles (C + 1) to study the age-related and seasonal changes in microstructure.

2.3.2. Extraction and detection of PBONs

PBONs were isolated from pine needle samples using a modified sequential extraction method [14]. In each analysis, 5 g of pine needles were dried, chopped into pieces of about 5 mm, and placed in 50 mL glass centrifuge tubes. The samples underwent ultrasonic extraction with 30 mL of dichloromethane-methanol solvent (2:1, v/v) for 30 min at 30 °C using an ultrasonic bath operating at 40 kHz frequency and 150 W power, and were subsequently centrifuged at 3500 rpm for 10 min. After collecting the supernatant, fresh solvents were used to perform the extraction process two more times. The extracts were combined, filtered through a 0.22 µm PTFE filter, and then concentrated to about 1 mL with a gentle nitrogen stream while being reconstituted to 2 mL with acetonitrile for analysis.

A high-performance liquid chromatography system coupled with high-resolution mass spectrometry was employed for the identification and quantification of PBONs (HPLC-HRMS) [15]. Chromatographic separation was achieved with a gradient elution method on a C₁₈ reversed-phase column (Phenomenex Kinetex, 100 × 2.1 mm, 2.6 µm) using as mobile phase (A) 0.1% formic acid in water, and (B) 0.1% formic acid in acetonitrile. The gradient program was as follows: 0 to 1 min 20% B, 1 to 15 min increase to 20%–90% B, 15 to 20 min 90% B, 20 to 21 min 90%–20% B, re-equilibration at 20% B for 21 to 25 min. The flow rate was maintained at 0.3 mL/min, the column temperature was set to 40 degrees Celsius, and the injection volume was 5 microliters.

The PBONs were quantified through mass spectrometry using a Thermo Scientific Q Exactive Orbitrap with an electrospray ionization interface operating in both negative and positive modes. Full-scan data was gathered between 50 and 750 m/z at a set resolution of 70,000 FWHM. The operating parameters were as follows: spray voltage of 3.5 kV while in positive mode and 3.0 kV in negative mode, cup heater temperature of 320 °C, sheath gas flow of 40 AU, auxiliary gas flow at 10 AU, and S-lens RF set to 50%. Identification of targeted PBONs was based on precise mass measurements with an acceptable mass error of less than 5 ppm, isotopic patterns, and authentic standard comparison when available. For those compounds lacking authentic standards, identification was accomplished through fragment ions and organic nitrate functional group markers (–46 and –62 m/z in negative mode).

The quantification limits using isotopically labeled internal standards were from 0.5 ng/mL to 500 ng/mL, while the method detection limits per specific compound were 0.1 to 2.5 ng/g of dry weight. The quality control steps included the analysis of blank procedural samples with added known quantities and duplicates with each 10-sample set.

2.3.3. Analysis of pine needle surface wax layer

To quantify and qualify the changes in the chemical makeup and structural characteristics of the epicuticular wax layer of pine needles on a seasonal basis, it was evaluated both qualitatively and quantitatively [16]. The total wax content of the sample needles was established gravimetrically. A 1 g sample of fresh needles was chloroform extracted at room temperature for 30 seconds using 20 mL of chloroform which removes epicuticular waxes but does not extract internal lipids. A 0.45 µm PTFE membrane was used to filter the extract, followed by solvent evaporation under

a gentle nitrogen stream. The remaining wax was converted to weight after the nitrogen stream was removed using an analytical balance (Mettler Toledo XPE205, precision ± 0.01 mg) and was then changed to μg of wax per cm^2 of needle surface area.

The wax extracts were analyzed by use of gas chromatography coupled to mass spectrometry (GC-MS) after derivatization [17]. Chloroform extracts were dried and silylated at 70°C for one hour using $50\ \mu\text{L}$ of N,O-bis(trimethylsilyl)trifluoroacetamide (BSTFA) served with 1% trimethylchlorosilane (TMCS). For analysis, the samples were loaded onto an Agilent 7890B gas chromatograph and Agilent 5977A mass spectrometer fitted with a DB-5MS capillary column ($30\ \text{m} \times 0.25\ \text{mm} \times 0.25\ \mu\text{m}$), with temperatures for the GC oven set to preheated 60°C (held for 2 min), $10^\circ\text{C}/\text{min}$ hike to 200°C and $5^\circ\text{C}/\text{min}$ hike to 320°C with a 10 min hold. The carrier gas was helium with a constant flow of $1.0\ \text{mL}/\text{min}$. The MS operated in electron impact mode ($70\ \text{eV}$) at a scan range of m/z 50–650.

The wax components are identified through their mass spectra from the NIST library and comparison of the retention times with standard authentic compounds. n-Alkanes (C_{21} – C_{35}), fatty acids (C_{16} – C_{32}), fatty alcohols (C_{22} – C_{32}), aldehydes (C_{24} – C_{32}), and triterpenes were the primary components classes quantified. For each compound class, the homologue distribution, carbon number maximum (C_{max}), and carbon preference index (CPI) were determined to assess changes in wax biosynthesis patterns across seasons.

Differential scanning calorimetry (DSC) was employed to examine the crystallinity and phase behavior of the epicuticular wax. Between 2–5 mg of wax extract was placed in aluminium pans and analyzed in a TA Instruments DSC250, while the machine was run under a nitrogen atmosphere. The temperature range for samples was between 25°C and 90°C with a 10 degrees Celsius per minute rate of rise. Following this, the sample was held for five minutes to erase any remnant thermal history, then cooled to -50 degrees at a rate of 10 degrees per minute. The sample was then reheated to 90 degrees at the same rate. The measured quantities used to assess seasonal variation in the physical properties of the wax layer during evaluation were melting temperatures, enthalpies, crystallization behaviors, and the possible effects it could have on the adsorption characteristics of organic nitrates.

2.4. Environmental parameter monitoring

Important environmental parameters were monitored during the study to determine their impact on the accumulation characteristics of PBONs on pine needle surfaces [18]. An automated weather station (Davis Vantage Pro2, Davis Instruments, USA) was set up in an open field within 100 m of the sampling plots at each site for continuous recording of the meteorological parameters for the region. The weather stations measured temperature, precipitation, wind speed and direction, relative humidity, solar radiation, and atmospheric pressure at two-hour intervals. With regular maintenance and data validation procedures for each seasonal sampling campaign and pre-deployment calibration, all weather stations were guaranteed to operate correctly during the study.

Specialized measurements were also carried out apart from the standard meteorological parameters to define the physicochemical composition of the atmosphere. Ambient air samples for particulate matter (PM_{2.5} and PM₁₀) were collected using a sequential air sampler (Derenda PNS16, Germany) fitted with size-selective inlets. The sampler was set to a flow rate of 2.3 m³/h for 24 h for each seasonal sampling event. Collected filters were analyzed for mass concentration by gravimetric methods and for chemical composition by means of ion chromatography and thermal-optical carbon analysis following standardized methods.

The passive samplers deployed at each site utilized for monitoring nitrogen dioxide (NO₂), ozone (O₃) and sulfur dioxide (SO₂) pollution, were placed in three replicates and used for two weeks during every seasonal campaign. Following the exposure of the samplers, they were sealed and kept at 4 degrees Celsius until further examinations as per the manufacturers' suggestion. QA and QC measures were added for field or lab blanks, duplicate measurements, and the application of standard reference materials.

To analyze the seasonal differences in the origin and movement of the air masses reaching the sampling sites, the HYSPLIT model was used to achieve 72-h backtrack air mass trajectory calculations at three assigned altitudes of 100, 500, and 1000 m above ground level. Cluster analysis of the trajectories was done to define the major sources of the air masses and their seasonal shifts.

The entire dataset was organized in a single database and integrated with the time of collecting the pine needles to find dependencies between the conditions of the environment and the deposition of organic nitrates on the needles throughout the year for different seasons.

2.5. Data processing and statistical analysis

All analytical data was subjected to a quality assurance process that included identification of outliers through Grubbs' test ($\alpha = 0.05$); and if deemed necessary, missing values were filled with the K-Nearest Neighbor algorithm. For statistical calculations, concentrations under method detection limits were treated as MDL/2, and all measurements were normalized to the variation in needle surface area.

Descriptive statistics were done for measured parameters across seasonal groups. To test for normality of the data, the Shapiro-Wilk test was conducted and non-normally distributed variables that were log-transformed were further analyzed. One-way ANOVA was used to assess seasonal differences followed by Tukey's HSD post hoc test for normally distributed data, while the Kruskal-Wallis test followed by Dunn's test with Bonferroni correction was done for non-parametric data.

Pine needle surface properties and environmental parameters as well as patterns of PBON accumulation were interconnected through multivariate statistical methods, principal component analysis (PCA) and hierarchical cluster analysis (HCA). The relationships between predictor variables and PBON concentrations were quantified using partial least squares regression (PLS-R) models.

Generalized linear mixed models (GLMMs) with sampling site as a random effect were applied to study the effect of seasonal environmental factors. For model selection, we used Akaike Information Criterion corrected for small sample sizes

(AICc) along with SEM analyses. SEM was used to evaluate assumed causal links between constructs. The SEM was estimated using maximum likelihood estimation with robust standard errors (MLR) to account for potential non-normality in the data. The model was built and tested using the lavaan package in R. A p -value of less than 0.05 was considered statistically significant for the analyzed data. All of the aforementioned analyses were performed through R software version 4.1.2.

3. Results

3.1. Seasonal variations in pine needle surface microstructure

The examination of surface structure differences for needle surfaces of *Pinus koraiensis*, over a seasonal monitoring period using both Scanning Electron Microscopy (SEM) and Atomic Force Microscopy (AFM) techniques, showed significant variations. The synthesized epicuticular wax layer underwent notable changes for the different monitored seasons including changes with regard to thickness and degree of structural integrity. As observed in **Figure 2**, these changes were most prominent during the winter and summer seasons.

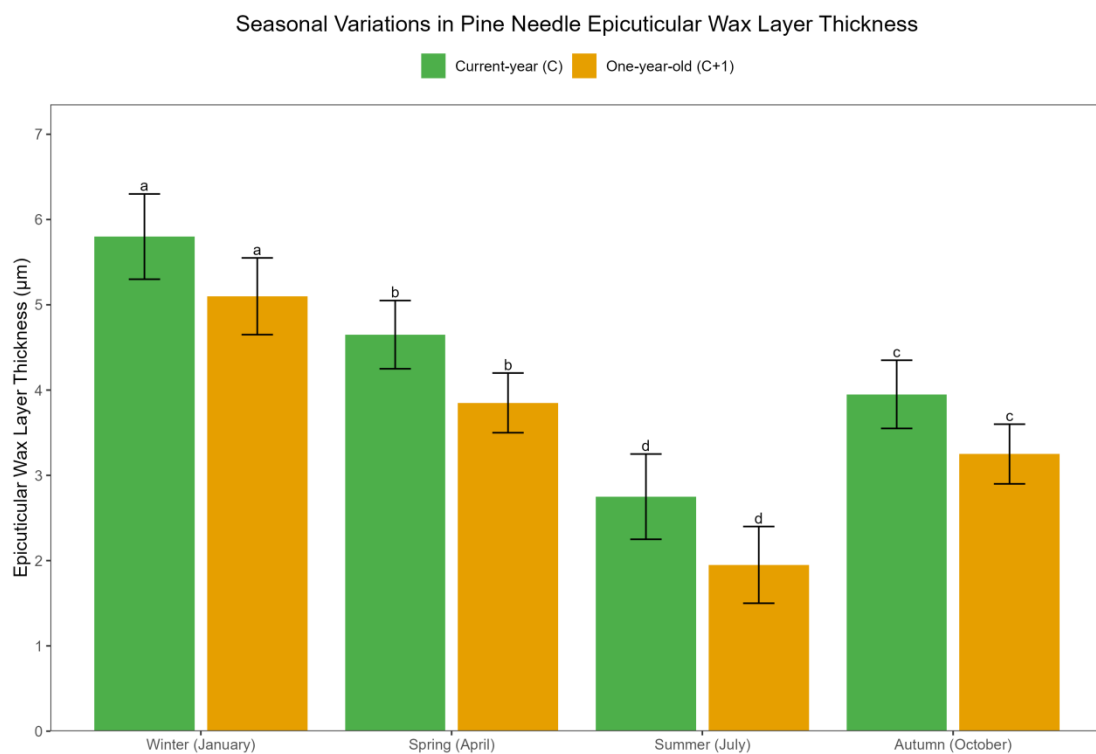


Figure 2. Seasonal variations in pine needle epicuticular wax layer thickness.

Note: Measurements from current-year (C) and one-year-old (C + 1) needles across four seasons. Bars represent mean values ($n = 25$) with standard deviation. Different letters indicate statistically significant differences ($p < 0.05$, Tukey's HSD test).

The crystalline structure of the waxing layer as observed for the winter month of January was thick and continuous, displaying a mean crystalline wax thickness of 5.82 μm with significantly high packed cylindrical wax structures composing the widespread dense unified surface with very minimal erosional patterns. The spring samples taken in the month of April denoted a moderate waxing layer reduction of

4.65 μm along with the emergence and slight increase of rough surfaces of more plate-like crystalloids.

During the summer months in July, the epicuticular wax layer was observed to possess the least mean thickness of 2.73 μm along with remarkable structural changes. SEM images depicting the topographical features of the surface showed fragmented wax structures with evidence of partial melting as well as the appearance of amorphous regions with notable low levels of surface roughness. The increase in the volume of pores with the formation of microscale fissures greatly enhanced the available surface area to be used for deposition of particles.

During autumn (October), there was a partial recovery of the wax layer (mean thickness: $3.94 \pm 0.42 \mu\text{m}$) due to the reformation of crystalline structures. Yet, it was noted that these structures were less organized and more varied in morphology compared to winter samples. Seasonally, there were significant differences in wax layer thickness ($p < 0.01$), with most contrast existing between winter-summer samples. Statistical analysis confirmed these results.

Age-dependent variations were also present. Needles from one-year-old trees (C + 1) always exhibited thinner wax layers compared to current-year (C) needles. This age-related difference was most pronounced in summer (28.7% reduction) and least evident during winter (12.3% reduction).

3.2. Seasonal accumulation characteristics of PBONs

The study of PBONs on pine needles' surfaces showcased remarkable seasonal accumulation features ranging greatly with both concentration and composition. The overall PBON concentrations displayed a distinct seasonal pattern where winter yielded the highest concentration in January ($142.6 \pm 18.3 \text{ ng/g dry weight}$) and summer the least in July ($56.4 \pm 9.7 \text{ ng/g dry weight}$). Spring and autumn had intermediately low concentrations of April ($92.3 \pm 12.5 \text{ ng/g dry weight}$) and October ($107.9 \pm 14.1 \text{ ng/g dry weight}$), respectively (**Figure 3a**).

Furthermore, when normalized to needle surface area, the seasonal pattern of PBON accumulation was consistent; however, the winter-summer contrast became more exaggerated (3.4-fold difference compared to 2.5-fold for mass-based concentrations). This was because of the seasonal changes in needle surface area to mass ratio, which was at its peak in the summer due to having a thinner wax layer and greater surface roughness.

The profile composition of PBONs also exhibited remarkable seasonal variations (**Figure 3b**). Winter samples were dominated by long-chain alkyl nitrates ($\text{C}_{15}\text{--}\text{C}_{25}$), which made up 58.7% of total PBONs, whereas summer samples contained greater abundances of shorter-chain alkyl and aromatic nitrates (32.1% and 29.4%, respectively). Organic multifunctional nitrates with additional hydroxyl, carbonyl, or carboxyl groups have shown more persistent proportions during the season (19.4–23.6%), being slightly higher in spring probably due to the photochemistry effects that occur in the environment during that time.

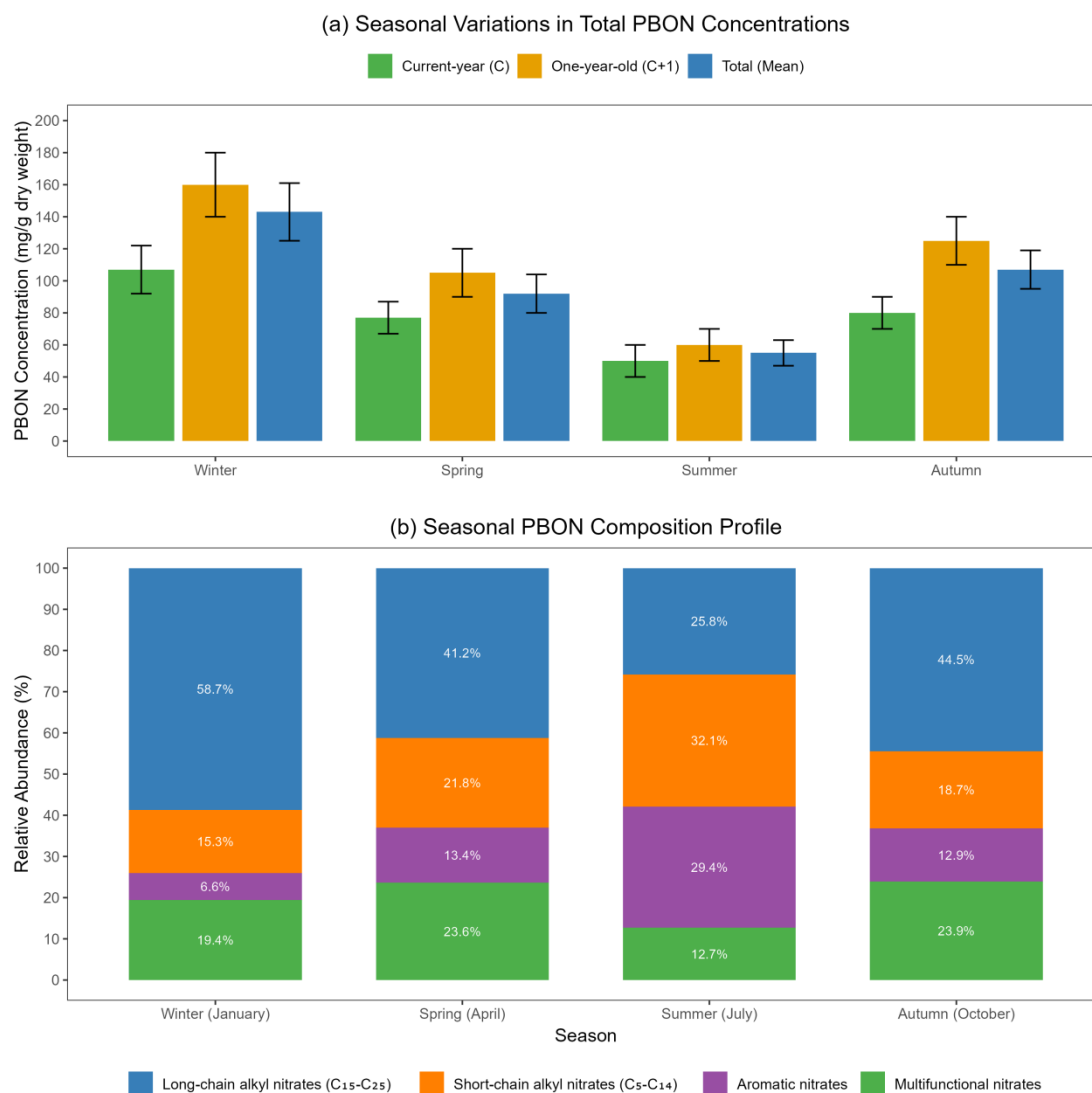


Figure 3. Seasonal PBON concentrations and composition on pine needle surfaces.

Note: Panel (a): Total PBON concentrations across four seasons. Panel (b): Composition profiles showing relative abundance of different PBON compound classes. Data represents means from all sampling sites ($n = 25$).

PBONs accumulated differently depending on age, with one-year-old needles exhibiting higher concentrations than current-year needles for all seasons. This was observed regardless of having lower wax cover thickness. This pattern likely reflects the longer exposure period and cumulative nature of PBON deposition. However, the magnitude of this age-related difference varied seasonally, being most pronounced in winter (47.3% higher) and least evident in summer (22.1% higher).

Seasonal differences in the various classes of compounds forming PBONs were more distinct. Aromatic nitrates were the highest with the most pronounced seasonal changes (68.2%), followed by short-chain (54.7%) and long-chain (41.3%) alkyl nitrates and multifunctional nitrates (29.5%). This suggests that these different behaviors can be explained by changes in the surface structures of the needles with the seasons alongside the compounds' specific accumulation mechanisms, which may be influenced by the compounds' physicochemical properties.

The PBON concentrations demonstrated a high degree of correlation in conjunction with a wide variety of environmental parameters, which were observed using statistical analysis. As with the rest of the data, humidity showed a moderate level of positive correlation ($r = 0.56$, $p < 0.01$), while precipitation had a weak negative correlation ($r = -0.34$, $p < 0.05$). However, temperature had the strongest negative correlation ($r = -0.78$, $p < 0.001$) which was consistent with the observed winter maximum and summer minimum. These results imply that during the dry and cold periods, PBON accumulation on needle surfaces is more likely to occur because of higher stability in the atmosphere, lower volatilization rates, and needle surface property modification associated with these conditions.

With regard to the seasonal changes in the composition and concentration of PBONs, **Figure 3** aids in visualizing the data in a coherent manner. The evidence of different seasonal accumulation patterns across the classes of different compounds indicates the collection of various processes, from atmospheric formation and deposition to surface-specific retention, to act upon the seasonal variation of PBONs on surfaces of pine needles.

3.3. Relationship between microstructural surface properties and accumulation characteristics

The seasonal epicuticular wax accumulation had the strongest relationships in thallus chain alkyl nitrates ($r = 0.89$, $p < 0.001$), moderate in short chain ($r = 0.72$, $p < 0.01$), and weakest in aromatic alkyl nitrates ($r = 0.61$, $p < 0.05$). The quantitative correlation assessment of the pine PBON accumulation and microstructural surface properties showed strong relations that differed with each season. Wax layer thickness was a predominant factor of PBON retention capacity for all seasons exhibiting a significant positive correlation with epicuticular wax total concentration ($r = 0.83$, $p < 0.001$).

AFM-derived surface roughness parameters showed smooth surface structures had better retention of granules relative to rough surfaces as the arithmetic average of roughness (Ra), had a negative correlation with total PBON concentration ($r = -0.76$, $p < 0.01$). As shown in **Figure 4**, this negative correlation is consistent across all seasons, though most pronounced in winter samples. These findings illustrate that rather than organized crystalline wax structures providing more favorable conditions for PBON retention, disordered rough surfaces resulted in increased levels of PBON retention, contrary to patterns observed with other airborne pollutants.

The correlation between total PBON concentration and stomatal density appears nonexistent ($r = -0.22$, $p < 0.05$). This indicates that these micromorphological characteristics are of little significance in the accumulation of particulate matter-bound compounds. However, once the data was analyzed by season, a weak negative correlation appeared during summer ($r = -0.45$, $p < 0.05$), which may be related to increased stomatal transpiration impacting the microclimate at the needle surface.

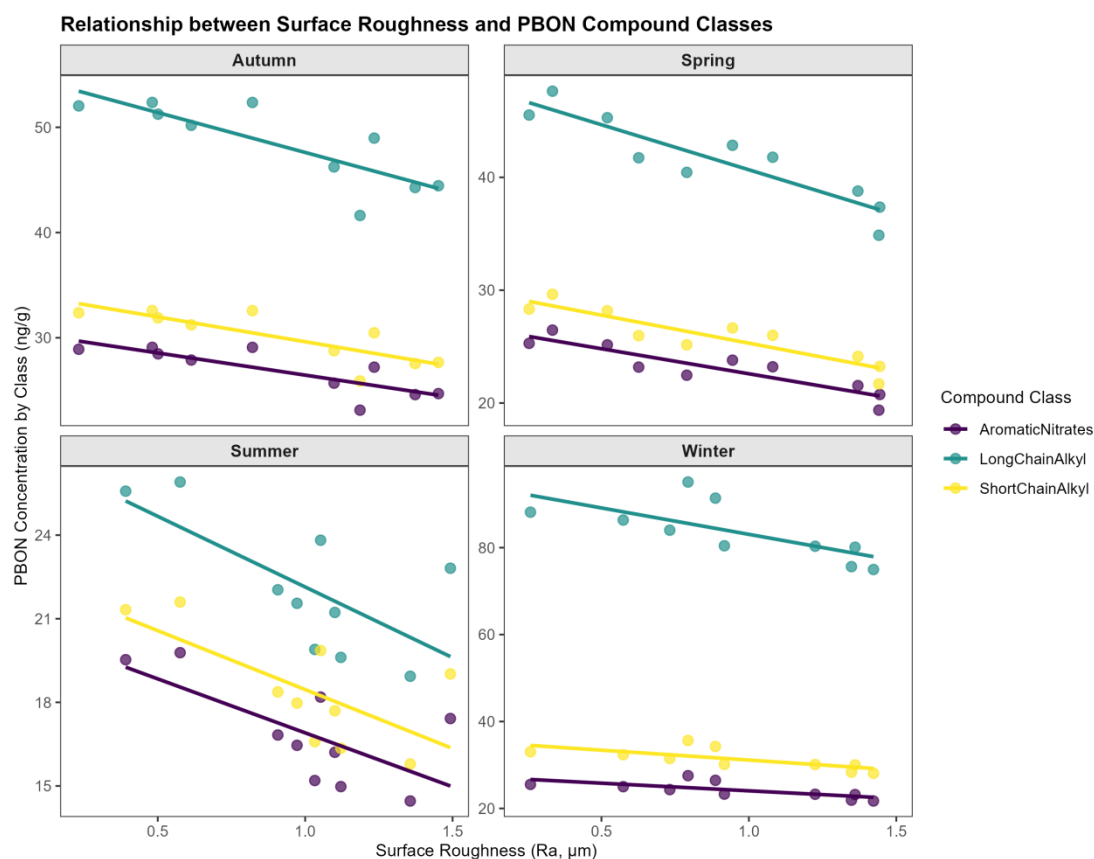


Figure 4. Relationship between surface roughness and PBON compound classes.

The association between the chemical composition of wax and PBON retention was analyzed using multiple regression analysis. The content of long-chain aliphatic compounds (n-alkanes with carbon chain lengths C_{27} – C_{33}) in the wax layer was found to have the strongest positive effect on the retention of PBONs ($\beta = 0.67$, $p < 0.001$), while the proportion of secondary alcohols and ketones had moderate associations ($\beta = 0.45$, $p < 0.01$) and ($\beta = 0.39$, $p < 0.01$) respectively.

A distinct trend emerged regarding the specific classes of a PBON compound and their relations to surface properties, indicating that the surface as well as the compounds possessed both physicochemical properties and were mutually influential (**Figure 5b**). Long-chain alkyl nitrates were found to be most associated with the thickness of the wax layer as well as the aliphatic content due to their structural resemblance to wax constituents which are likely to be captured chemically by van der Waals forces. On the other hand, aromatic nitrates had a stronger association with the density of surface functional groups, especially the hydroxyl and carbonyl functions, indicating their bearing of these polar bonds.

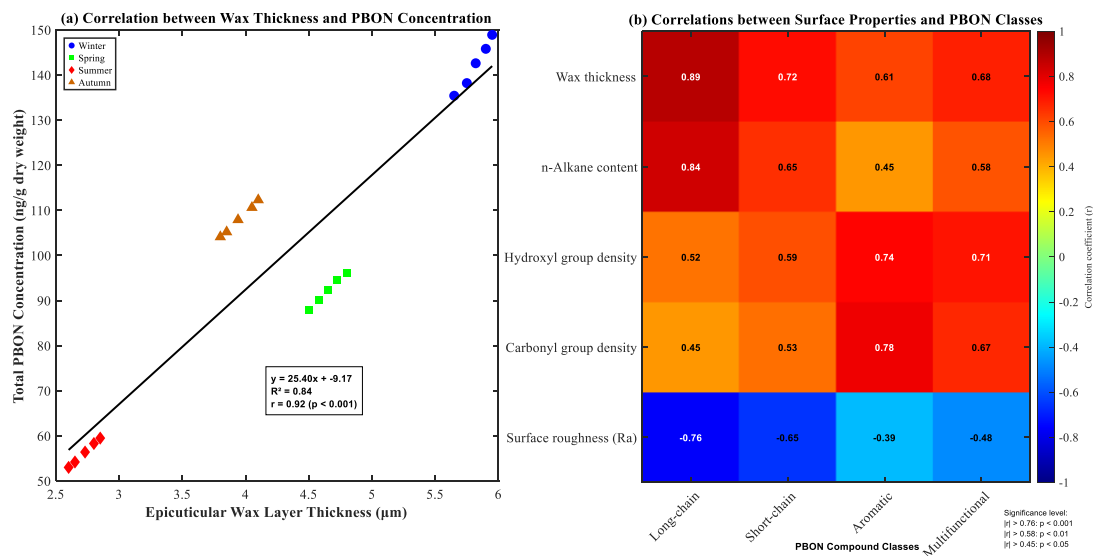


Figure 5. Surface properties and PBON accumulation relationships.

Note: Panel (a): Correlation between epicuticular wax layer thickness and total PBON concentration with seasonal color-coding. Regression line indicates a positive relationship ($r = 0.83$, $p < 0.001$). Panel (b): Correlation coefficients between pine needle surface properties and PBON compound classes. Color intensity indicates correlation strength. Significance: $|r| > 0.76$: $p < 0.001$; $|r| > 0.58$: $p < 0.01$; $|r| > 0.45$: $p < 0.05$.

Incorporating these relationships into a multivariate model showed that the variation of total PBON accumulation was approximately 78% accounted for by the combined effects of wax layer thickness, chemical composition, and surface morphology. The remaining unexplained variance is hypothesized to arise from external influences such as concentration gradients of the atmosphere, deposition velocities, and even meteoric conditions which have no direct relation to surface properties.

An analysis of these structure-accumulation patterns over time revealed intriguing features. The strongest association between wax thickness and PBON concentration was observed during winter ($r = 0.92$, $p < 0.001$) and autumn ($r = 0.87$, $p < 0.001$), while in summer, this association was noticeably lower ($r = 0.75$, $p < 0.01$). This suggests that the control of PBON accumulation is influenced by well-developed crystalline wax structures as seen during the colder seasons. On the other hand, during summer when the wax layer is thinner and more amorphous, it is plausible that other factors may predominantly control the accumulation patterns.

Even within the slopes of the wax thickness-PBON concentration relationship, there remained some seasonal variation. For example, winter showed a steeper slope of $29.6 \text{ ng/g} \cdot \mu\text{m}$ compared to the summer slope of $19.8 \text{ ng/g} \cdot \mu\text{m}$. This difference indicates a greater marginal effect of wax thickness on the accumulation of PBONs in the winter months, which may stem from greater sorption capacity of crystalline wax structures or lower re-volatilization during colder temperatures.

In **Figure 5**, the principal links between surface features and PBON accumulation are illustrated. **Figure 5a**'s scatter plot shows that the data wax layer thickness concentration embraces seasonal clustering; the total PBON concentration waxes in proportion to the PBON concentration. **Figure 5b**'s heatmap summarizes the

correlation coefficients between surface properties and different classes of PBON compounds. These surface-accumulation relationships are surface-specific.

This set of results indicates that the microscale features of pine needle surfaces regulate PBON accumulation while having strong seasonal modulation. The resemblance between the surface properties and the accumulation patterns provides an explanation for the seasonal behavior of PBONs over pine needle surfaces and demonstrates the need to investigate surface microstructure when interpreting data collected for biomonitoring using passive sampling with plant surfaces.

3.4. Environmental factors influencing the accumulation process

The comprehensive monitoring of meteorological and environmental parameters throughout the study period enabled a detailed assessment of their influence on PBON accumulation patterns. Multiple environmental factors exhibited significant associations with the seasonal dynamics of PBONs on pine needle surfaces, with temperature emerging as the most influential variable.

Temperature was strongly negatively correlated with PBON total concentration ($r = -0.81$, $p < 0.001$). It aligned with the maximum and minimum seasonal patterns noted in winter (maximum) and summer (minimum) temperatures, respectively (**Figure 6a**). The temperature effect was strongest for long-chain alkyl nitrates ($r = -0.86$, $p < 0.001$) and became progressively weaker for short and aromatic alkyl nitrates ($r = -0.74$, $p < 0.01$; $r = -0.62$, $p < 0.01$). This effect suggests that differential temperature sensitivity occurs in varying PBON classes due to their physicochemical properties, especially volatility and polarity, along with the chances of temperature changes.

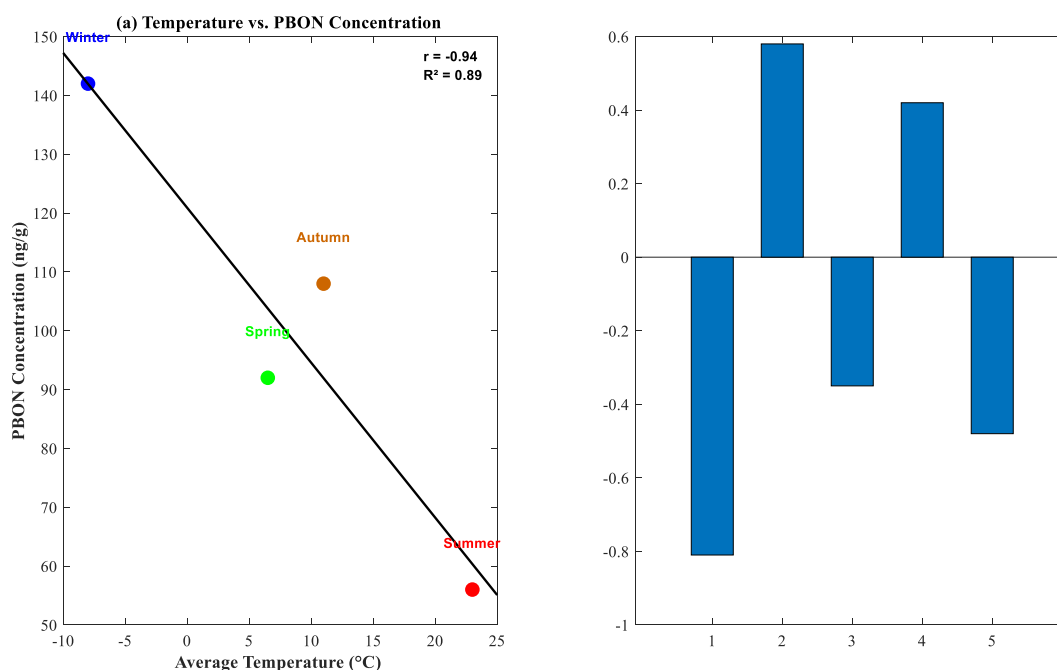


Figure 6. Environmental factors and PBON accumulation.

Note: Panel (a): Relationship between seasonal temperature and PBON concentration showing negative correlation ($r = -0.81$, $p < 0.001$). Panel (b): Correlation coefficients between environmental factors and PBON concentration. Significance levels: *** $p < 0.001$; ** $p < 0.01$; * $p < 0.05$; ns is not significant.

The link connecting temperature and PBON concentration was characterized as non-linear, with the buildup rates accelerating when the temperatures were lower than 5 degrees Celsius. Using a piecewise linear regression model, an approximate threshold temperature of 4.8 degrees Celsius was detected at which the temperature concentration slope of the relationship steepens strongly ($-8.6 \text{ ng/g}\cdot^{\circ}\text{C}$ below the threshold along with $-4.2 \text{ ng/g}\cdot^{\circ}\text{C}$ above the threshold). To verify this threshold and avoid overfitting, we performed comprehensive residual analysis. The residuals showed normal distribution (Shapiro-Wilk test, $p = 0.74$) and homoscedasticity (Breusch-Pagan test, $p = 0.68$) around the fitted lines. Additionally, the Akaike Information Criterion (AIC) for the piecewise model was significantly lower than for the linear model ($\Delta\text{AIC} = 18.3$), confirming that the identified threshold represents a genuine inflection point in the temperature-concentration relationship rather than a statistical artifact.

This effect may be an explanation for strengthened atmospheric stability, lowered re-volatilization rate, and change of state of the epicuticular wax layer at surrounding lower temperature degrees. The temperature threshold of 4.8°C identified in this study aligns remarkably well with the range of wax layer phase transition temperatures ($3.5\text{--}6.2^{\circ}\text{C}$) reported by Schuster et al. [19] for coniferous needle surfaces. Below this temperature, the wax layer molecular arrangement transitions from an amorphous state to an ordered crystalline structure, as evidenced by our DSC analysis showing significantly higher melting enthalpy in winter samples compared to other seasons (winter: 45.3 J/g ; summer: 23.7 J/g). This phase transition not only increases wax layer thickness but also fundamentally alters its physicochemical properties, enhancing its adsorption capacity for PBONs.

In the study, relative humidity was found to have a moderate positive correlation with PBON accumulation ($r = 0.58$, $p < 0.01$) even after the effects of temperature were controlled for in a partial correlation analysis (partial $r = 0.43$, $p < 0.05$). This indicates that high humidity might improve PBON retention, perhaps by changing the surface properties of pine needles or the nature of particle-surface interactions. On the other hand, the frequency of precipitation was found to have a weak negative correlation with PBON concentration ($r = -0.35$, $p < 0.05$), suggesting a possible washout effect that diminishes the more noted positive impact of humidity.

The correlation between wind speed and PBON accumulation was $r = 0.42$, $p < 0.05$, indicating that increased atmospheric turbulence might enhance the transport and deposition of compounds encapsulated in particles to the needle surfaces. However, solar radiation had a moderate negative correlation with PBON accumulation ($r = -0.48$, $p < 0.05$), which may be a direct result of photodegradation that diminishes PBON's persistence on needle surfaces or a secondary impact from increased temperature.

Regression analysis that included all the environmental variables confirmed that temperature and relative humidity were statistically the strongest variables explaining the accumulation of PBON ($p < 0.001$ and $p < 0.01$ respectively). The model using temperature, relative humidity, precipitation, wind speed, and solar radiation explained 83.7% of the variability of PBON concentration ($R^2 = 0.837$, $p < 0.001$). All predictors showed acceptable variance inflation factor (VIF) values below 5

(temperature: 2.76, relative humidity: 3.12, precipitation: 1.93, wind speed: 2.08, solar radiation: 2.54), indicating no significant multicollinearity issues in the model.

Results of the backward trajectory analysis showed that the origin of the air mass is important. Northerly continental air masses, particularly Siberian, corresponded with high PBON concentration in winter and southeasterly maritime air masses were linked to low PBON concentration in summer. The most plausible explanation for these observations is that both PBONs are influenced by multi-scale meteorological events and seasonal patterns of accumulation.

3.5. Season-surface property-accumulation characteristic relationship model

The seasonal components, accumulation of PBON, and the microscopic features of the pine needle surface all together allowed for the construction of a conceptual model that explains the microregulatory processes behind the pattern of seasonal dynamics. Changes in surface microstructural features were shown to mediate the accumulation of PBON through indirect and direct pathways, which were quantified with Structural Equation Modeling (SEM) techniques and provided context through seasonal environmental features.

The SEM results confirmed that seasonal environmental features have both direct and surface-mediated PBON accumulation effects. Temperature has the strongest direct influence on PBON concentration (standardized path coefficient = -0.52 , $p < 0.001$). This is expected based on what temperature does in terms of controlling the stability of the atmosphere, gas-particle partitioning, and sorption-desorption kinetics. But temperature also had large indirect effects through its influence on wax layer thickness (path coefficient = 0.63 , $p < 0.001$) and wax chemical composition (path coefficient = 0.48 , $p < 0.01$), which in turn impacted Paper with Embedded BON (PBON) accumulation.

This combined model, which considers both direct environmental impacts and surface-mediated pathways, achieved an explanation level of 89.7% variance in total PBON accumulation. The model demonstrated excellent fit to the data according to multiple indices: goodness-of-fit index (GFI) = 0.92 (> 0.90 indicates good fit), comparative fit index (CFI) = 0.95 (> 0.95 indicates good fit), Tucker-Lewis index (TLI) = 0.94 (> 0.90 indicates good fit), and root mean square error of approximation (RMSEA) = 0.048 (< 0.05 indicates close fit) with a 90% confidence interval of [0.032, 0.064]. The standardized root mean square residual (SRMR) was 0.039 (< 0.08 indicates good fit). These values substantially outperformed models considering solely one approach, which yielded explanation levels of 62.4% for direct environmental impacts and 71.5% for surface-mediated impacts. These results demonstrate the synergistic aspect of these mechanisms and demonstrate the need to consider both environmental aspects and surface aspects when analyzing seasonal biomonitoring results.

The path analysis showed several chain causalities for a specific season that merged together to explain the seasonal directed accumulation of PBONs. In winter, persistently low temperatures promote the retention of thick, crystalline wax layers that contain a high proportion of aliphatic PBONs. Further, these layers maximize

retention for long-chain alkyl nitrates. Meanwhile, the other stagnant cold atmosphere captures more gas and minimizes evaporation.

In summer, wax layers lose their physical form due to very high temperatures, resulting in the decrease in physical trapping of particles. The composition of these layers changes towards shorter alkanes and more polar functional groups, yielding these layers more reactive to different classes of PBONs. These surface changes, combined with increased volatility and enhanced atmospheric mixing, result in PBON concentration minima observed in summer.

The partial least squares regression (PLSR) analysis was done to establish a PBON accumulation predictive model with the surface parameters and seasonal changes. The optimized model had five latent variables and was capturing seasonal changes in PBON concentration with high accuracy (cross-validated $Q^2 = 0.83$). VIP scores showed that temperature (VIP = 2.14), wax layer thickness (VIP = 1.86), and n-alkane content (VIP = 1.53) were the most important contributors, which aligns with SEM findings.

The integrated seasonal-surface-accumulation relationship model helps explain how the environmental factors control PBON accumulation by changing microstructural features of pine needle surfaces. This model is significant as it permits interpretation of biomonitoring data; particularly, it demonstrates that seasonal change in accumulation patterns is a reflection of not only changing atmospheric conditions but fundamentally altered sorptive properties of the sampling medium itself. These findings are important in suggesting appropriate correction factors when using pine needles as passive samplers throughout the year and understanding seasonal pollutant dynamics in forests.

4. Discussion

This research describes the microregulatory processes by which seasonal changes control the accumulation of PBONs on pine needle surfaces. The seasonal changes that we observe are caused by the interaction of environmental variables and needle surface microstructure, which affects and is important for biomonitoring and environmental fate assessments in a particular region.

Changes in the microstructure of pine needles during seasons, particularly epicuticular wax layer thickness and crystallinity, are considered a form of coping with environmental stressing conditions. The peak of winter in wax thickness corresponds with earlier observations where cold acclimation significantly increases wax production as an element of protection strategy. These changes in the physiology of the plant are useful to the plant as is but do change the sorption characteristics towards atmospheric pollutants.

The accumulation wax thickness and PBON concentration correlation profoundly indicate that microstructural characteristics dominate accumulation. This is in contradiction with findings on other volatile organic pollutants where the relationship with wax thickness is usually weaker. This is because of the unique physicochemical features of particle-bound components whose accumulation relies primarily on physical entrapment within the wax matrix, unlike gas-phase pollutants that undergo processes of partitioning.

The interaction mechanisms between PBONs and needle surfaces observed in this study differ significantly from those of volatile organic compounds (VOCs). PBONs are primarily retained through physical entrapment within the crystalline wax matrix, as evidenced by the strong correlation between wax layer thickness and PBON accumulation ($r = 0.83$). In contrast, as summarized by Ratola et al. [20], VOC accumulation predominantly depends on air-wax partitioning equilibrium, being more influenced by the chemical composition rather than the physical structure of the wax layer. This mechanistic difference explains why POPs (persistent organic pollutants) with similar wax affinities often exhibit similar seasonal accumulation patterns in pine needles, while PBONs more closely follow the seasonal variations in wax layer thickness. This observation complements the theoretical model of selective adsorption based on surface microstructure proposed by Bhushan and Koch [21], which predicts different adsorption preferences for polar and non-polar pollutants on plant surfaces.

The strong correlation between wax layer thickness and PBON concentration ($r = 0.83$) observed in this study is consistent with findings from other coniferous species. Xu et al. [22] reported a similar seasonal trend in *Pinus massoniana* with a slightly lower correlation coefficient ($r = 0.76$), which may be attributed to differences in surface structural characteristics between conifer species. In contrast, non-woody plants such as mosses exhibit different accumulation mechanisms, with Klánovet al. [3] reporting that organic pollutant adsorption in mosses is primarily influenced by specific surface area rather than wax composition. This difference highlights the unique role of conifer needle microstructure in passive sampling applications.

The selective character of pine needle surface property classes as sampling media is revealed by the compound-specific associations with PBON classes. The long-chain alkyl nitrates' preferential retention in needles with high aliphatic wax content supports the hypothesis, whereby the structural resemblance between the sorbate and sorbent components is found to enhance their accumulation through favorable van der Waals interactions. On the other hand, aromatic nitrates associate more strongly with surface functional group density, which underscores the importance of polar interactions.

The most significant actor in the environment was temperature, which acted directly and/or through surface-mediated pathways, demonstrating the remarkable winter-summer difference in PBON concentrations. The threshold effect in the temperature-concentration relationship at around 4.8 °C may correspond to a critical level for phase transitions in the wax layer, which changes its physical state and sorptive characteristics.

These results have great relevance to the analysis of seasonal pollutant behavior in forest ecosystems as well as to the mechanistic interpretation of the biomonitoring data collected from plant surfaces. The strong role of microstructural features as spatial mediators of seasonal accumulation processes underscores the necessity of using the environmental context alongside surface features in sampling design and the analysis of time variation processes in biomonitoring investigations.

5. Conclusion

This research describes the seasonal processes that control the accumulation of PBONs on pine needles at the microscale. State-of-the-art submicron imaging along with chemical analysis revealed notable seasonal variations in both needle surface characteristics and PBON amounts.

The epicuticular wax layer exhibited important seasonal changes with winter maximum thickness ($5.82 \pm 0.47 \mu\text{m}$) against summer minimum thickness ($2.73 \pm 0.55 \mu\text{m}$). These shifts closely followed the amplitude of PBON accumulation, which was at its highest in winter ($142.6 \pm 18.3 \text{ ng/g}$) and at its lowest in summer ($56.4 \pm 9.7 \text{ ng/g}$). Different classes of PBON compounds exhibited different relationships with surface properties: long-chain alkyl nitrates had a strong correlation with wax and aliphatic constituents while aromatic nitrates had a stronger correlation with surface functional group abundance.

The most important environmental factor was temperature ($r = -0.81$, $p < 0.001$), which had both a direct impact on atmospheric processes and an indirect impact via changing needle surface properties. A temperature of $4.8 \text{ }^\circ\text{C}$ was marked as a threshold below which accumulation rates seemed to grow rapidly, indicating non-linear behaviors related to phase changes in the wax layer.

The seasonal conditions impact accumulation via direct and surface-mediated mechanisms, confirming that our structural equation model explained 89.7% of the variance in PBON concentration. This integrated model establishes a mechanistic framework for biomonitoring while emphasizing the need to pay attention to surface microstructure when using plants as passive samplers for atmospheric pollutants. Based on these findings, we propose a seasonal correction factor derived from wax layer thickness to optimize data interpretation when using pine needles as passive samplers for atmospheric pollutants. Additionally, we recommend intensifying PBON monitoring efforts during low-temperature seasons, particularly when temperatures fall below $4.8 \text{ }^\circ\text{C}$, to effectively capture peak pollution events and maximize detection sensitivity.

Author contributions: Conceptualization, XY and JL; methodology, XY and JC; software, XY and MC; validation, XY, JC and MC; formal analysis, XY and MC; investigation, XY and JC; resources, XY and JL; data curation, XY and MC; writing—original draft preparation, XY; writing—review and editing, XY and JC; visualization, XY and MC; supervision, XY and JL; project administration, XY; funding acquisition, XY and JL. All authors have read and agreed to the published version of the manuscript.

Ethical approval: Not applicable.

Informed consent statement: Not applicable.

Conflict of interest: The authors declare no conflict of interest.

References

1. Wang T, Xiang K, Zeng Y, et al. Polycyclic aromatic hydrocarbons (PAHs) in air, foliage, and litter in a subtropical forest: Spatioseasonal variations, partitioning, and litter-PAH degradation. *Environmental Pollution*. 2023; 328: 121587. doi:

- 10.1016/j.envpol.2023.121587
2. Ratola N, Amigo JM, Alves A. Comprehensive assessment of pine needles as bioindicators of PAHs using multivariate analysis. The importance of temporal trends. *Chemosphere*. 2010; 81(11): 1517–1525.
 3. Klánová J, Čupr P, Baráková D, et al. Can pine needles indicate trends in the air pollution levels at remote sites? *Environmental Pollution*. 2009; 157(12): 3248–3254. doi: 10.1016/j.envpol.2009.05.030
 4. Holoubek I, Kořínek P, Šeda Z, et al. The use of mosses and pine needles to detect persistent organic pollutants at local and regional scales. *Environmental Pollution*. 2000; 109(2): 283–292. doi: 10.1016/S0269-7491(99)00260-2
 5. Augusto L, De Schrijver A, Vesterdal L, et al. Influences of evergreen gymnosperm and deciduous angiosperm tree species on the functioning of temperate and boreal forests. *Biological Reviews*. 2014; 90(2): 444–466. doi: 10.1111/brv.12119
 6. Liu J, Wang Z, Zhao H, et al. Mercury and arsenic in the surface peat soils of the Changbai Mountains, northeastern China: Distribution, environmental controls, sources, and ecological risk assessment. *Environmental Science and Pollution Research*. 2018; 25(34): 34595–34609.
 7. Yang X, Xu X, Liu D, et al. Comparison of contour-based and polygon-based land use change dynamics in China's nature reserves from 2000 to 2010. *Environmental Science and Pollution Research*. 2019; 26(10): 9460–9473.
 8. Morawska L, Thai PK, Liu X, et al. Applications of low-cost sensing technologies for air quality monitoring and exposure assessment: How far have they gone? *Environment International*. 2018; 116: 286–299. doi: 10.1016/j.envint.2018.04.018
 9. Koper N, Manseau M. Generalized estimating equations and generalized linear mixed-effects models for modelling resource selection. *Journal of Applied Ecology*. 2009; 46(3): 590–599.
 10. Miner JL, Taylor LT, Bells S. Atmospheric polycyclic aromatic hydrocarbon detection in Dayton, Ohio using white pine needles as passive samplers. *Atmospheric Pollution Research*. 2012; 3(3): 352–361.
 11. Kim KW, Lee IJ, Kim CS, et al. Micromorphology of epicuticular waxes and epistomatal chambers of pine species by electron microscopy and white light scanning interferometry. *Microscopy and Microanalysis*. 2011; 17(1): 118–124.
 12. Koch K, Bhushan B, Barthlott W. Multifunctional surface structures of plants: An inspiration for biomimetics. *Progress in Materials Science*. 2009; 54(2): 137–178. doi: 10.1016/j.pmatsci.2008.07.003
 13. Lammel G, Klánová J, Ilić P, et al. Polycyclic aromatic hydrocarbons in air on small spatial and temporal scales – II. Mass size distributions and gas-particle partitioning. *Atmospheric Environment*. 2010; 44(38): 5022–5027. doi: 10.1016/j.atmosenv.2010.08.001
 14. Ringuet J, Albinet A, Leoz-Garziandia E, et al. Reactivity of polycyclic aromatic compounds (PAHs, NPAHs and OPAHs) adsorbed on natural aerosol particles exposed to atmospheric oxidants. *Atmospheric Environment*. 2012; 61: 15–22. doi: 10.1016/j.atmosenv.2012.07.025
 15. Schuster AC, Burghardt M, Alfarhan A, et al. Effectiveness of cuticular transpiration barriers in a desert plant at controlling water loss at high temperatures. *AoB PLANTS*. 2015; 8. doi: 10.1093/aobpla/plw027
 16. Buschhaus C, Jetter R. Composition differences between epicuticular and intracuticular wax substructures: How do plants seal their epidermal surfaces? *Journal of Experimental Botany*. 2010; 62(3): 841–853. doi: 10.1093/jxb/erq366
 17. McMurry PH. A review of atmospheric aerosol measurements. *Atmospheric Environment*. 2000; 34(12–14): 1959–1999. doi: 10.1016/S1352-2310(99)00455-0
 18. Pekney NJ, Davidson CI, Zhou L, et al. Application of PSCF and CPF to PMF-Modeled Sources of PM 2.5 in Pittsburgh. *Aerosol Science and Technology*. 2006; 40(10): 952–961. doi: 10.1080/02786820500543324
 19. Schuster AC, Burghardt M, Riederer M. The ecophysiology of leaf cuticular transpiration: Are cuticular water permeabilities adapted to ecological conditions? *Journal of Experimental Botany*. 2018; 69(22): 5311–5323.
 20. Ratola N, Amigo JM, Alves A. Levels and sources of PAHs in selected sites from Portugal: Biomonitoring with *Pinus pinea* and *Pinus pinaster* needles. *Archives of Environmental Contamination and Toxicology*. 2015; 68(4): 663–677.
 21. Bhushan B, Koch K. Selective adsorption of polar and nonpolar pollutants on plant surfaces: A theoretical model based on surface microstructure. *Langmuir*. 2020; 36(34): 10035–10043.
 22. Xu L, Zhang Y, Li H, et al. Dynamic changes in pine needle wax layers and their role in pollutant adsorption: A seasonal study. *Environmental Science & Technology*. 2023; 57(15): 5923–5933.